

On the complex solution of the Schrödinger equation with exponential potentials

Javier Garcia^{1, a)}

¹*Instituto de Física La Plata, Consejo Nacional de Investigaciones Científicas y Técnicas, and Departamento de Física, Universidad Nacional de La Plata, C.C. 67, 1900 La Plata, Argentina*

(Dated: 14 September 2023)

We study the analytical solutions of the Schrödinger equation with a repulsive exponential potential λe^{-r} , and that with an exponential wall λe^r , both with $\lambda > 0$. We show that the complex eigenenergies obtained for the latter tend either to those of the former, or to real rational numbers as $\lambda \rightarrow \infty$. In the light of these results, we explain the wrong resonance energies obtained in a previous application of the Riccati-Padé method to the Schrödinger equation with a repulsive exponential potential, and further study the convergence properties of this approach.

^{a)}jgarcia@fisica.unlp.edu.ar

I. INTRODUCTION

Resonances are solutions of the Schrödinger equation that have complex energies and present a purely outgoing behavior in the asymptotic region. These states, introduced by Siegert to describe decaying nuclear states using a stationary-state picture¹, arise, together with bound and virtual states (i.e., states that grow exponentially in the asymptotic region), as poles of the scattering matrix. They spark a lot of interest among physicists and chemists, evidenced by the large amount of methods devised for their computation. Most of them are based on the complex rotation method, introduced by Aguilar, Balslev, and Combes^{2,3}, which consists in performing a dilation on the coordinate $U(\theta)rU^{-1}(\theta) = e^{i\theta}r$, by choosing the parameter θ in such a way that the outgoing-wave state is transformed into one that asymptotically decays to zero, as bound states do, and then using one of the many numerical methods devised to compute the latter. The first applications of the complex rotation method involved a variational approach, which remains popular (e.g. Refs. 4–6) but also different techniques have been employed, such as numerical integration methods^{7–10}, dimensional scaling¹¹, the Lanczos’ Tau method¹², spherical-box approaches^{13,14}, direct computation of the Jost function¹⁵, gradient optimization¹⁶, and eigenvector continuation¹⁷, among others. There is also a wide array of methods that do not involve a complex rotation; examples of these include methods based on Siegert pseudo-states^{18–21}, the complex absorbing potential^{22,23}, Padé approximations of the S-matrix²⁴, the real stabilization method²⁵, the coupled channels method²⁶, and the Riccati-Padé method (RPM)^{27,28}. The list of methods provided here is by no means comprehensive.

The RPM consists in expanding a modified logarithmic derivative of the wavefunction in a Taylor series, and constructing Hankel determinants with the expansion coefficients, the roots of which give rise to sequences that converge rapidly towards both the bound states and resonances^{29,30}. It was originally proposed for the computation of bound states, but later it was found that it is also able to yield resonances without resorting explicitly to a complex rotation^{27,28}. Several applications to the computation of resonances ensued^{31–37}, which showed that it is able to compute them very accurately and with comparatively little cost. For example, the resonances for the Stark effect in the hydrogen atom computed by us in Ref. 37 are to our knowledge the most accurate available in literature.

As with bound states, there are very few systems whose resonances can be computed

analytically. One of such systems are the s -states of a particle exposed to a decaying exponential potential, i.e., $V(r) = \lambda e^{-r}$, with real λ . If $\lambda < 0$, the system admits a finite number of bound states^{38,39}. On the other hand if $\lambda > 0$, the potential is not expected to hold bound or resonant states, but some of the eigenfunctions, which correspond to complex eigenvalues, behave as such⁹. In addition, the repulsive exponential potential has a set of virtual states. The authors of Ref. 9 studied the complex eigenstates of the complex exponential potential both analytically and by means of the complex rotation method, and soon after the eigenvalues were used as benchmarks to test a few of the other numerical methods mentioned in the present work^{11,12,27,31}. Among these is the RPM, which produced some baffling results: it yields complex energies that are very close to those of the analytical solutions, but are not quite the same, unlike the approaches of Refs. 9, 11, and 12, which yielded the correct ones. The wrong results provided by the RPM were later confirmed in a more systematic study of the same problem³⁴. Ref. 31 also saw wrong results for the Schrödinger equation with the one-dimensional potential $V(x) = (x^2 - 2J) \exp(-\lambda x^2)$, introduced by Moiseiev to model pre-dissociation resonances of diatomic molecules⁴⁰, but it was later explained in Ref. 36 that the incorrect eigenvalues can also be obtained by complex rotation, provided that the rotation angle is set to be greater than the critical value $\theta_{\text{crit}} = \pi/4$. In fact, such eigenvalues had already been obtained and discussed by other authors^{7,8,41,42}. It is reasonable to expect that the discrepancy between the exact complex eigenenergies for the repulsive exponential potential and those obtained by the RPM can be explained in a similar fashion to those for the potential introduced in Ref. 40. In the present work, we show that this assumption is correct, and that the seemingly wrong resonances obtained by means of the RPM are in fact complex solutions of the Schrödinger equation for a particle exposed to an infinite exponential well, $V(r) = \lambda e^r$. Even though the latter has been solved analytically¹⁰, to our knowledge, both spectra have not yet been compared.

This work is organized as follows. In Sec. II, we review the analytical solution of the Schrödinger equation for both problems, and we perform a comparison between their eigen-spectra. Then, in Sec. III, we employ an efficient implementation of the RPM to improve upon the computations of Refs. 27, 31, and 34, and we study the rate of convergence of the roots of the Hankel determinants towards both kinds of complex eigenvalues. We finally sum up our results and draw further conclusions in Sec. IV.

II. ANALYTICAL TREATMENT

The Schrödinger equation with a repulsive exponential potential

We first treat the Schrödinger equation with a repulsive exponential potential,

$$-\phi''(r) + \lambda e^{-r}\phi(r) = \varepsilon\phi(r), \quad (1)$$

with $\lambda > 0$ and $\phi(0) = 0$. As discussed in the Introduction, this problem was already studied in Ref. 9 in great detail, but for consistency, we briefly describe its analytical solution in the following paragraphs.

By defining $\mu = \sqrt{-4\varepsilon}$, Eq. (1) is exactly solvable in terms of the Bessel functions of the first kind $J_{\pm\mu}(z)$, where $z = 2\sqrt{-\lambda}e^{-r/2}$ ^{9,38}, or, equivalently, in terms of the modified Bessel functions of the first kind $I_{\pm\mu}(t)$, where $t = 2\sqrt{\lambda}e^{-r/2}$. We prefer the latter since for real r , t is also real, whereas z is imaginary. The general solution of Eq. (1) can be written as $A_{\mu}I_{\mu}(t) + B_{\mu}I_{-\mu}(t)$, and the condition that $\phi(r)$ behaves as an outgoing wave, i.e., $\phi(r) \sim e^{ikr}$, with $k = i\mu/2$, $\text{Re}(k) > 0$ and $\text{Im}(k) < 0$ ⁹, which implies $\text{Re}(\mu) < 0$ and $\text{Im}(\mu) < 0$, requires that $B_{\mu} = 0$, since for small $|t|$, $I_{\pm\mu}(t) \sim (t/2)^{\pm\mu}/\Gamma(\mu + 1)$. The condition $\phi(0) = 0$ results in

$$I_{\mu_n}(2\sqrt{\lambda}) = 0, \quad (2)$$

which yields the eigenvalues $\varepsilon_n = -\mu_n^2/4$. Here $n = 0, 1, \dots$ serves as a label that orders them by increasing absolute value. It is well known that the solutions of Eq. (2) are either real and negative or come in complex conjugate pairs, with $\text{Re}(\mu) < 0$ ⁹. For $\lambda \rightarrow 0$, they tend to negative integers, and as λ increases, pairs of solutions coalesce to form a complex pair, one pair at a time. The solutions with real $\mu < 0$ correspond to virtual states, i.e., states that grow exponentially as $r \rightarrow \infty$, and the complex solutions correspond to either resonances, if $\text{Im}(\mu) < 0$, or growing states $\text{Im}(\mu) > 0$. Since the roots of Eq. (2) come in complex conjugate pairs, every resonance comes with an associated growing state. In the present work, the notation μ_n will refer only to resonances. If needed, the associated growing states will be referred to by using complex conjugation, i.e. μ_n^* .

The authors of Ref. 9 were limited to solving Eq. (2) for relatively small values of λ , since it was easier for them to find its roots by means of the computational resources that were available at that time. Contrarily, nowadays they are quite trivial to find with any number

of significant digits by using any modern computer algebra software, or a multiprecision library such as `mpmath`⁴³, which we have used extensively in the present work.

The Schrödinger equation with an infinite exponential well

We now focus our attention on the Schrödinger equation with an infinite exponential well potential, i.e.,

$$-\phi''(r) + \lambda e^r \phi(r) = \epsilon \phi(r). \quad (3)$$

It is related to Eq. (1) by a change of variable $r \rightarrow -r$, and it is also solvable in terms of Bessel functions, as was shown by Atabek and Lefebvre in Ref. 10. They posed Eq. (3) as a three-parameter problem, with $V(r) = Ae^{\alpha(r-r_0)}$, but by making the change of variable $r \rightarrow r/\alpha$, setting $\lambda = A \exp(-\alpha r_0)/\alpha^2$, and multiplying the energy by α^2 , Eq. (3) is obtained without loss of generality. In the present work we would like to provide an equivalent derivation of its analytical solution that we deem more adequate for the ensuing discussion.

The general solution of Eq. (3) can be written $A_\nu I_\nu(s) + B_\nu K_\nu(s)$, where $s = 2\sqrt{\lambda}e^{r/2}$, and K_ν is the modified Bessel function of the second kind, defined for noninteger ν as $K_\nu(s) = \pi \csc(\nu\pi)[I_{-\nu}(s) - I_\nu(s)]/2$, and for integer n , $K_n(s) = \lim_{\nu \rightarrow n} K_\nu(s)$. It could also be written in terms of $I_{\pm\nu}(s)$, but we choose K_ν instead since for $|s| \rightarrow \infty$ they admit the following asymptotic expansions,

$$I_\nu(s) \sim \left(\frac{1}{2\pi s}\right)^{1/2} e^s \left[1 - \frac{4\nu^2 - 1}{8z} + \frac{(4\nu^2 - 1)(4\nu^2 - 9)}{2!(8z)^2} + \dots\right] \quad (4)$$

$$K_\nu(s) \sim \left(\frac{\pi}{2s}\right)^{1/2} e^{-s} \left[1 + \frac{4\nu^2 - 1}{8z} + \frac{(4\nu^2 - 1)(4\nu^2 - 9)}{2!(8z)^2} + \dots\right], \quad (5)$$

Eq. (4) is valid only when $-\pi/2 < \arg s < \pi$, whereas Eq. (5) is valid in the range $-\pi < \arg s < \pi$. For real r (and, consequently, real s) the decaying eigenfunctions of Eq. (3) require $A_\nu = 0$, and the condition $\phi(0) = 0$ implies

$$K_\nu(2\sqrt{\lambda}) = 0, \quad (6)$$

which yields the bound states. For $\lambda > 0$, there is an infinite amount of roots of Eq. (6), and all of them are all imaginary^{44–46}, which implies that the spectrum is comprised of an infinite number of positive energies. The eigenfunctions are strongly decaying for $r \rightarrow \infty$, since $\phi(r) \sim \sqrt{\pi/\sqrt{\lambda}} \exp[-2e^{r/2}\sqrt{\lambda} - r/4]$.

We now study the solutions to Eq. (3) under a complex rotation of the form $r = \rho e^{i\theta}$, with $(\rho, \theta) \in \mathbb{R}$. We focus on the interval $(-\pi/2, \pi/2)$ since when $\theta = \pm\pi/2$, the asymptotic behavior of the solutions changes drastically, as r becomes imaginary. In fact, as $|\theta| > \pi/2$, the real part of r changes sign, and the problem could be reinterpreted as that of Eq. (1), but with $r = \rho e^{i\theta'}$, and $\theta' = \pi - \theta$; we may therefore define $\theta_{\text{crit}} = \pi/2$ as the critical complex rotation angle for which the infinite well is transformed into the finite repulsive exponential potential. The complex-rotated s can be written as

$$s = 2\sqrt{\lambda} e^{\frac{1}{2}\rho \cos \theta} e^{\frac{1}{2}i\rho \sin \theta}, \quad (7)$$

and, since $\arg s = \rho \sin(\theta)/2$, it becomes apparent that not only does $\arg s$ change with θ , but also with ρ . When $|\rho \sin \theta| > \pi$, Eq. (4) is no longer valid, and when $|\rho \sin \theta| > 2\pi$, Eq. (5) becomes invalid, as well. To circumvent this problem, we resort to the analytical continuation formulae for the modified Bessel functions⁴⁷,

$$I_\nu(se^{m\pi i}) = e^{m\nu\pi i} I_\nu(s) \quad (8)$$

$$K_\nu(se^{m\pi i}) = e^{-m\nu\pi i} K_\nu(s) - \pi i \sin(m\nu\pi) \csc(\nu\pi) I_\nu(s), \quad (9)$$

where $m = 0, \pm 1, \pm 2, \dots$. Eqs. (8) and (9) can be employed to extend the validity of Eqs. (4) and (5) to regions where $\arg s$ is greater than $\pi/2$. For example, if ρ and θ are such that $\pi/2 < \arg s < 3\pi/2$, then by setting $m = -1$ in Eqs. (8) and (9), the argument of $se^{m\pi i}$ stays within the region $(-\pi/2, \pi/2)$. In general, for any given value of ρ , an integer m can be chosen such that $\arg(se^{m\pi i})$ lies between $-\pi/2$ and $\pi/2$, both for positive and negative θ . If λ is large enough, the RHS of Eq. (9) is expected to behave as an asymptotically decaying function if

$$-(1 + 2m)\pi < \rho \sin \theta < -(1 - 2m)\pi, \quad (10)$$

where m and θ have opposite signs. Eq. (6) is now generalized,

$$e^{-m\nu_n^{(m)}\pi i} K_{\nu_n^{(m)}}(2\sqrt{\lambda}) - \pi i \sin[m\nu_n^{(m)}\pi] \csc[\nu_n^{(m)}\pi] I_{\nu_n^{(m)}}(2\sqrt{\lambda}) = 0, \quad (11)$$

where again we use n as a label for the eigenvalues, according to their increasing absolute value, and now the value of m is added as a parenthesized superindex. The energy of each state is computed as $\epsilon_n^{(m)} = -[\nu_n^{(m)}]^2/4$. When $m = 0$ we recover Eq. (6), but when $m \neq 0$, a different set of complex solutions is obtained. Since for real x , $[I_\nu(x)]^* = I_{\nu^*}(x)$, and

Symbol	Meaning
μ_n	Solutions of Eq. (2), ordered by increasing absolute value. If μ_n is complex, $\text{Im } \mu_n < 0$.
$\nu_n^{(m)}$	Solutions of Eq. (11), ordered by increasing absolute value.
$\nu_{n^*}^{(m)}$	Solution of Eq. (11) that is closest to μ_n .
$\epsilon_n, \epsilon_n^{(m)}, \epsilon_{n^*}^{(m)}$	$-\mu_n^2/4, -[\nu_n^{(m)}]^2/4, -[\nu_{n^*}^{(m)}]^2/4$.
$\tilde{\epsilon}_n, \tilde{\epsilon}_n^{(m)}, \tilde{\epsilon}_{n^*}^{(m)}$	Roots of H_D^d closest to $\epsilon_n, \epsilon_n^{(m)}$, and $\epsilon_{n^*}^{(m)}$.
$\Delta_n, \Delta_n^{(m)}, \Delta_{n^*}^{(m)}$	$-\log_{10} \epsilon_n - \tilde{\epsilon}_n , -\log_{10} \epsilon_n^{(m)} - \tilde{\epsilon}_n^{(m)} , -\log_{10} \epsilon_{n^*}^{(m)} - \tilde{\epsilon}_{n^*}^{(m)} $.

TABLE I. Summary of notation.

$[K_\nu(x)]^* = K_{\nu^*}(x)$, by taking the complex conjugate of Eq. (11), it can be readily seen that $\nu_n^{(-m)} = [\nu_n^{(m)}]^*$.

Eq. (11) generalizes Eqs. (25), (28) and (32) of Ref. 10. The equivalence of both approaches is made more apparent by substituting the definition of K_ν in terms of $I_{\pm\nu}$ into Eq. (11) and dividing by $e^{m\nu\pi i}$, whereas we obtain

$$\csc(\pi\nu) \left[e^{m\nu\pi i} I_{-\nu}(2\sqrt{\lambda}) - e^{-m\nu\pi i} I_\nu(2\sqrt{\lambda}) \right] = 0, \quad (12)$$

[in the comparison, note that $I_\nu(z) = e^{\mp\nu\pi i/2} J_\nu(ze^{\pm\pi i/2})$]. The factor $\csc(\pi\nu)$ cannot be overlooked since it becomes singular when ν is an integer number. It is also apparent from Eq. (12) that if ν_n is a solution, $-\nu_n$ is one as well, which is to be expected since only ν^2 appears in the Schrödinger equation. To simplify the upcoming discussions, we will refer to the resonances that correspond to the complex solutions of Eq. (2) as “barrier resonances”, (even though the repulsive exponential potential is not a barrier, the complex solutions of that problem behave as it were) and to those that correspond to Eqs. (11) and (12) as “well resonances”. We may as well refer to Eq. (1) as the “barrier problem”, and to Eq. (3) as the “well problem”. The notation we employ to distinguish between the solutions of Eqs. (1) and (3), as well as the one we use to refer to the quantities computed in Sec. III, is summarized in Table I.

Comparison of both spectra

We now focus on comparing the well and barrier resonances. To that end, we have computed the well resonances for λ ranging from 0.1 to 12, and $m = 1, 2, 3, 4$. We have also computed the barrier resonances for the same values of λ ; both kinds are shown in Fig. 2 (the barrier resonances are the same for each plot, since they do not depend on m). It can

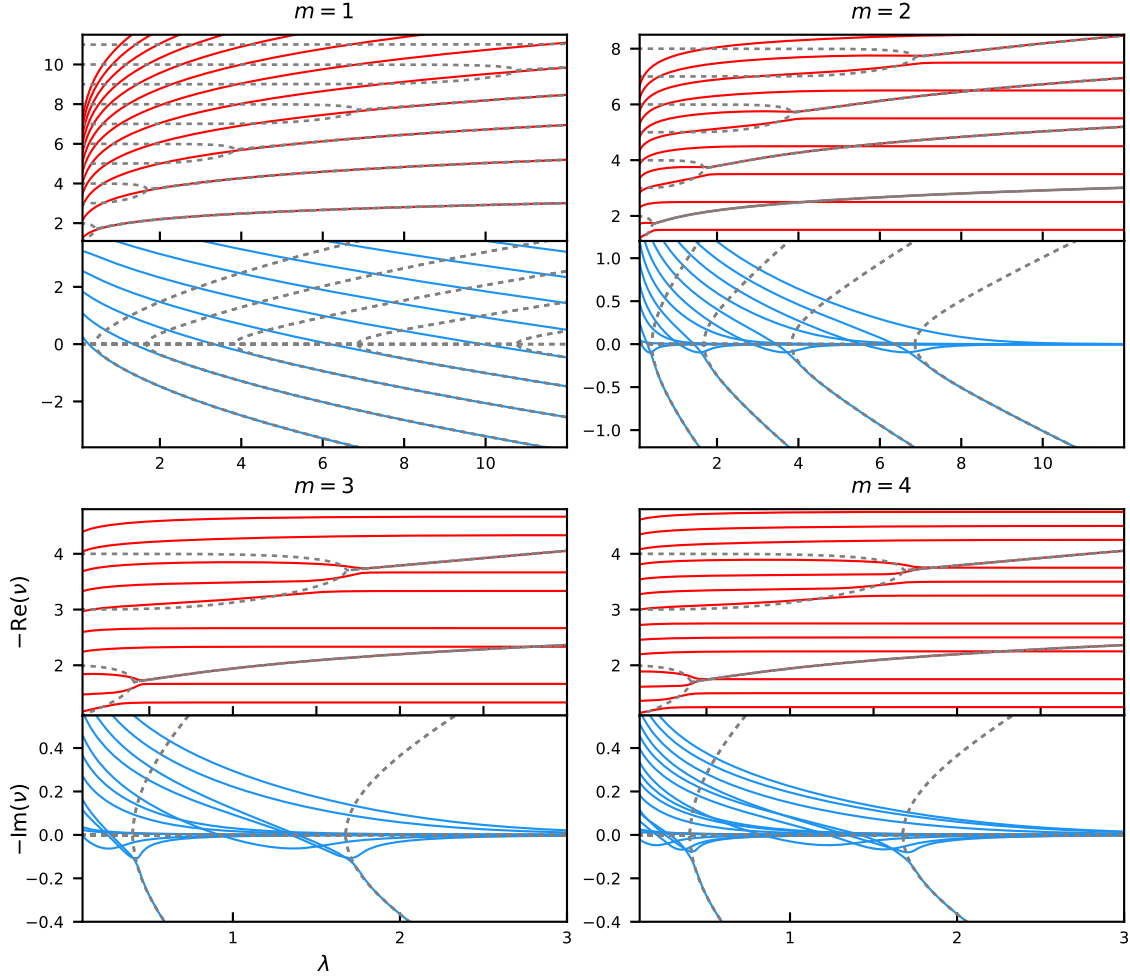


FIG. 1. Real and imaginary parts of the well resonances for $m = 1, 2, 3$, and 4 [Eq. (11), solid lines], and of the barrier resonances [Eq. (2), dashed lines].

be seen that for increasing λ , when $m = 1$, all of the well resonances converge towards the growing-state barrier ones. For $m = 2$, half of the well resonances converge towards barrier resonances, whereas the other half appear to converge to semi-integer numbers. Following this trend, for $m = 3$, one every three well resonances converge towards barrier resonances, whereas the other two converge towards fractions of 3 (excluding integers), and for $m = 4$, one in four well resonances converge towards barrier resonances. It is apparent that the well resonances can be divided into two kinds; the first kind involves those solutions that converge towards barrier resonances, whereas the second kind involves those well resonances that converge towards fractional numbers, and are only present for $m > 1$. We will not provide

$\lambda = 1/2$			$\lambda = 2$		
m	$\text{Re}(\nu)$	$\text{Im}(\nu)$	m	$\text{Re}(\nu)$	$\text{Im}(\nu)$
1	-1.708889402333520	0.313848239102419	1	-2.19998150521571	1.47380332298928
2	-1.746877069032750	0.289471834435959	2	-2.19996056123564	1.47382974620043
3	-1.744703781423560	0.280605627380309	3	-2.19996055822964	1.47382974508387
4	-1.743009480401320	0.281164740911281	4	-2.19996055822965	1.47382974508356
5	-1.743125645499290	0.281441559500668	∞	-2.19996055822965	1.47382974508356
6	-1.743171729577290	0.281420065685151			
7	-1.743167735582120	0.281412353572321			
8	-1.743166449785450	0.281413091451232			
9	-1.743166585008590	0.281413305242469			
			$\lambda = 10$		
m	$\text{Re}(\nu)$	$\text{Im}(\nu)$	m	$\text{Re}(\nu)$	$\text{Im}(\nu)$
10	-1.743166620466710	0.281413280623280	1	-2.91772003768616	4.57704829026394
11	-1.743166616009740	0.281413274758419	2	-2.91772003768629	4.57704829026402
12	-1.743166615042500	0.281413275561234	∞	-2.91772003768629	4.57704829026402
13	-1.743166615186450	0.281413275720256			
14	-1.743166615212510	0.281413275694549			
15	-1.743166615207940	0.281413275690295			
			$\lambda = 100$		
m	$\text{Re}(\nu)$	$\text{Im}(\nu)$	m	$\text{Re}(\nu)$	$\text{Im}(\nu)$
16	-1.743166615207250	0.281413275691106	1	-4.32572713644441	17.46003535736490
17	-1.743166615207390	0.281413275691218	∞	-4.32572713644441	17.46003535736490
18	-1.743166615207410	0.281413275691193			
19	-1.743166615207400	0.281413275691190			
20	-1.743166615207400	0.281413275691191			
∞	-1.743166615207400	0.281413275691191			

TABLE II. $\nu_{1^*}^{(m)}$, and μ_0 (denoted with $m = \infty$) for different values of λ . See Table I for the definition of each symbol.

rigorous proof, but the existence of both kinds of solutions can somewhat be explained by analyzing Eq. (12). First, we note that, provided that λ is large enough, because of Eq. (5), $K_\nu(2\sqrt{\lambda})$ is a complex number of very small magnitude. In addition, for $\text{Im}(\nu_n^{(m)}) < 0$ and $m > 0$, $e^{-m\nu\pi i}$ has also a very small magnitude. Therefore, it can be expected that the zeros of Eq. (11) will be close to those of $\sin(m\nu\pi) \csc(\nu\pi) I_\nu(2\sqrt{\lambda})$. The latter can occur either if $I_\nu(2\sqrt{\lambda}) = 0$, which implies that $\nu_n^{(m)} \approx \mu_n$ (this explains the first kind of resonances), or if $\sin(m\nu\pi) \csc(\nu\pi) = 0$, which occurs whenever $\nu = k/m$, where k is an integer that is not a multiple of m (explaining the second kind).

In Table II, we show $\nu_{0^*}^{(m)}$, where the index n^* refers to the solution of Eq. (11) that is closest to μ_n , for several values of λ and for increasing m . It can be seen that the distance between $\nu_{n^*}^{(m)}$ and μ_n becomes smaller with increasing λ , but also with m . We further

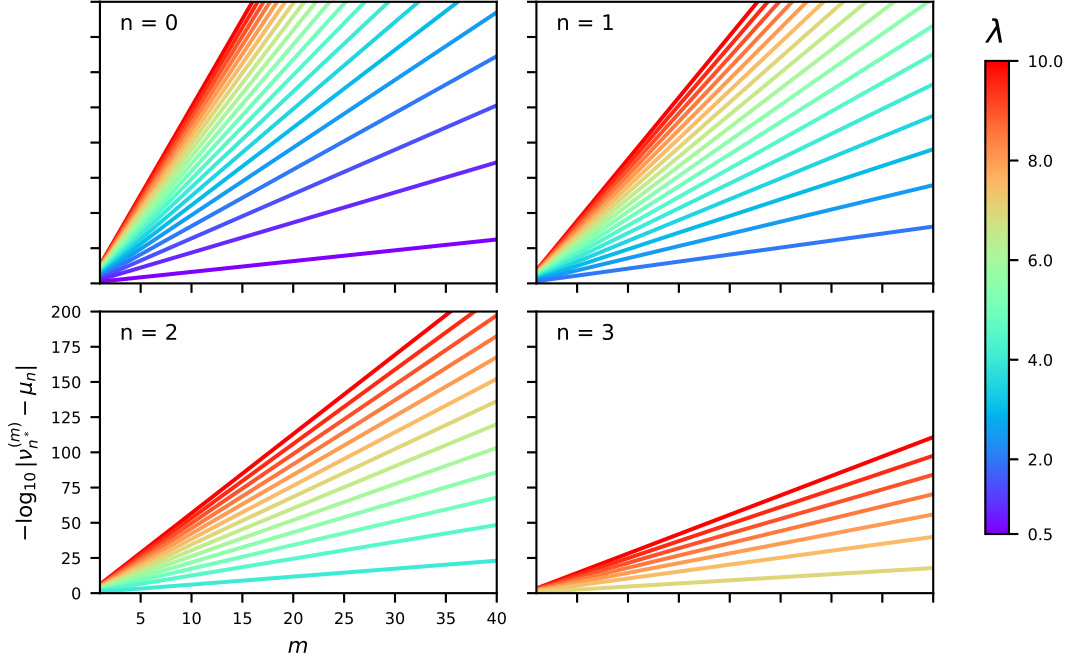


FIG. 2. Logarithmic difference between the roots of Eqs. (2) and (11).

demonstrate the latter by showing in Fig. 2 the computation of $-\log_{10} |\mu_n - \nu_n^{(m)}|$, for $n = 1, \dots, 4$, and several values of λ ranging from 1/2 to 10. It can be seen there that for fixed λ and increasing m , the distance between the well and barrier resonances decreases exponentially. In fact, one can show that

$$\nu^{(m)} - \mu \approx i \frac{K_\mu}{\pi \dot{I}_\mu} e^{-i\mu\pi(2m-1)}, \quad (13)$$

where $\dot{I}_\mu = (\partial I_\nu / \partial \nu)|_{\mu=\nu}$, by expanding the LHS of Eq. (11) a Taylor series about $\nu = \mu$ [where μ is a root of Eq. (2)], keeping the linear term, and assuming that the term involving \dot{I}_μ is much larger (in the asymptotic sense) than those involving K_μ and \dot{K}_μ . Although Eq. (13) is not proved rigorously, we have performed several computations that confirm it numerically.

Going back to the barrier problem [Eq. (1)], one may wonder if a similar set of solutions such as those of Eq. (11) may be discovered through complex rotation, since if $r = \rho e^{i\theta}$ is substituted in the definition of t , it follows that $\text{Arg } t = -\rho \sin(\theta)/2$; i.e., $\text{Arg } t$ changes with ρ , thereby modifying the asymptotic behavior of the solution depending on the region where the boundary condition is imposed, just as in the case of the well problem. The answer is

that it would not, since, even though an equation analogous to (10) might be posed for the barrier problem, the analytical continuation of I_ν is proportional to the same function [see (8)]; the set roots of an equation equivalent to (11) are then the same for every m .

III. RICCATI-PADÉ METHOD

The purpose of the present section is to apply the RPM to both Eqs. (1) and (3). The application of the RPM to central-force problems was presented in Ref. 29, but for completeness we briefly review it here.

The RPM can be applied to any central-force problem, i.e.,

$$-\psi''(r) + \left[V(r) + \frac{l(l+1)}{r^2} - E \right] \psi(r) = 0, \quad (14)$$

with $\psi(0) = 0$, and $\psi(\infty) = 0$, where the potential $V(r)$ can be expanded in a Laurent series of the form $\sum_{j=-1}^{\infty} v_j r^j$. In that case, $\psi(r) \sim Cr^{l+1}$ for $r \rightarrow 0$, and its logarithmic derivative is singular at origin, $\psi'(r)/\psi(r) \sim (l+1)/r$; therefore it must be regularized. The resulting regularized function, $f(r) = (l+1)/r - \psi'(r)/\psi(r)$, can then be expanded in a Taylor series about the origin, $f(r) = \sum_{j=0}^{\infty} f_j r^j$. It is a solution to the Riccati equation,

$$f'(r) - f^2(r) + \frac{2(l+1)}{r} f(r) - [E - V(r)] = 0, \quad (15)$$

from which a recurrence relation can be found for the f_j coefficients,

$$f_{j+1} = \frac{1}{2l+j+3} \left[\sum_{i=0}^j f_i f_{j-i} - v_j + E\delta_{j0} \right], \quad (16)$$

with $f_0 = -v_{-1}/(2l+2)$. $f(r)$ can also be approximated by a Padé approximant of order $[M/N]$, i.e., a quotient of polynomials of orders M and N that are typically chosen in such a way that $[M/N](r) - f(r) = \mathcal{O}(r^{M+N+1})$. If the condition $[M/N](r) - f(r) = \mathcal{O}(r^{M+N+2})$ is imposed instead, it leads to a system of equations that has nontrivial solutions if

$$|H(D, d)| = \begin{vmatrix} f_{d+1} & f_{d+2} & \cdots & f_{d+D} \\ f_{d+2} & f_{d+3} & \cdots & f_{d+D+1} \\ \vdots & \vdots & \ddots & \vdots \\ f_{d+D} & f_{d+D+1} & \cdots & f_{2D+d-1} \end{vmatrix} = 0. \quad (17)$$

Here we have defined $d = M - N$ and $D = N + 1$. The Hankel determinants [the determinants of $H(D, d)$] can be computed efficiently by resorting to the following recurrence relation,

$$H_D^d = \frac{H_{D-1}^d H_{D-1}^{d-2} - (H_{D-1}^{d+1})^2}{H_{D-2}^{d-2}}, \quad (18)$$

where $H_D^d = |H(D, d)|$, with $H_0^d = 1$.

The RPM is closely related to the process of sending a movable pole at infinity⁴⁸. This pole can be moved through any ray in the complex plane, and for this reason the solutions of Eq. (17) yield approximations to the eigenvalues of Eq. (14) whose corresponding eigenfunctions that asymptotically decay through different regions of the complex plane. Concordantly, the roots of Eq. (17) persist if a complex rotation of the variable is performed³⁶. Another important characteristic of the RPM is that H_D^d typically exhibits a great number of roots in the neighborhood of each eigenvalue; this makes it easier to differentiate the roots that approximate an eigenvalue from those that are spurious, but it also complicates the task to find the optimal sequence of roots that converges to each eigenvalue by means of iterative methods.

Application to the present problem

In the present work we have employed two different approaches to compute the roots of Eq. (17). The first of them is to compute an expression for H_D^d analytically, and solve for E using a polynomial root-finding algorithm; in this way, all of the roots of H_D^d can be found for a given D , but it is only applicable to small D values, since the degree of H_D^d grows rapidly. The second one is to use the recurrence relation (18) to compute H_D^d and its derivative numerically, and to employ the Newton-Raphson (NR) to find its roots. It has the advantage of being extremely efficient, but only one root can be computed at a time, and a good initial value of the energy is required for the NR method to converge. Since the Hankel determinants present clusters of roots that approach the eigenvalues, it is not guaranteed that the NR method will find the optimal one, but with large D , even the suboptimal sequences of roots provide a good approximation to the eigenvalues. We are typically able to compute determinants with $D \leq 30$ with the first approach before running out of memory, whereas with the second one, we have reported results with $D > 800$ ⁴⁹, and even larger determinants are possible, provided that the starting points for the NR method are sufficiently accurate. We would like to mention here that we have utilized the GiNaC library^{50,51} for the implementation of the second approach.

By setting $V(r) = \lambda e^{\pm r}$, and $l = 0$, Eq. (14) yields Eq. (1) or (3). The choice of the sign in $V(r)$ is irrelevant since, as stated earlier, the roots of H_D^d remain unmodified. Since

the results obtained by the RPM do not typically change with d , we have set $d = 0$ in all of our computations. We have computed all of the roots of H_{30}^0 , and selected the ones that coincide with the exact eigenvalues of both Eqs. (1) and (3); these are shown, for $\lambda = 1/2$, in Table III, and, for $\lambda = 10$, in Table IV. It can be appreciated that some of them approach the bound states, and others approach the barrier and well resonances, but none of them are close to any of the virtual states. For both values of λ , the bound states and resonances corresponding to $m = 1$ are found with more significant digits than those with $m = 2$, and in the latter case, there is also one root that corresponds to an $m = 3$ resonance. Among the results presented in Table III is included the seemingly wrong ground state for the exponential barrier, $E \approx -0.705450568055028 + 0.268165964871580i$, found in Ref. 34. This value coincides with $-\nu_{1*}^{(1)2}/4$, where $\nu_{1*}^{(1)}$ is taken from Table II. The first root with $m = 1$, and the second one with $m = 2$ of Table III may also be considered as approximations towards $\varepsilon_0(\lambda = 1/2) \approx -0.73985 - 0.2452i$, whereas the third entries of Table IV for $m = 1, 2$ may be considered as approximations towards $\varepsilon_0(\lambda = 10) \approx 3.10907 - 6.6772i$. We also note here that the roots of Eq. (17) are either real or come in complex conjugate pairs, since the v_j coefficients of Eq. (16) are real, the f_j coefficients are polynomials on E with real coefficients, and so is H_D^d ; therefore, the same analysis performed here is valid for the growing-state solutions.

It is expected that for increasing D , the accuracy of these results will improve, but also that there will be roots of H_D^0 that approach the well resonances with $m \geq 4$. Since the computation of the whole set of roots of H_D^d becomes expensive for $D > 30$, in order to study how rapidly the roots of H_D^d converge towards both the barrier and well resonances, we have resorted to our NR-based approach. With it, we have computed $\tilde{\epsilon}_n^{(m)}$, which is the root of H_D^0 closest to $\epsilon_n^{(m)}$, and $\tilde{\epsilon}_n$, the root of H_D^0 closest to ε_n , for $D = 5, 10, \dots, 500$, $m = 0, \dots, 4$, $n = 0, \dots, 7$, and $\lambda = 1/2, 10$. We have employed the exact resonance energies computed from Eqs. (2) and (11) as a starting point for the NR method. Instead of showing the tens, or even hundreds, of coincident significant digits between the exact eigenvalues and their RPM approximations, we illustrate how accurate the latter are by means of the quantities $\Delta_n^{(m)}(D) = -\log_{10} |\tilde{\epsilon}_n^{(m)}(D) - \epsilon_n^{(m)}|$, and $\Delta_n(D) = -\log_{10} |\tilde{\epsilon}_n(D) - \varepsilon_n|$, both of which provide a good estimate of the number of correct decimal places. The plots of $\Delta_n^{(m)}(D)$ and $\Delta_n(D)$ are shown in Fig. 3; the latter labeled as $m = \infty$. It can be seen there that $\Delta_n^{(m)}(D)$ are straight lines whose slopes depend on m , but not on n . The position of these

m	$\text{Re}(\epsilon)$	$\text{Im}(\epsilon)$
0	3.2292159472536048534	0.0
0	7.0837240758343799367	0.0
0	11.541280962123897449	0.0
0	16.53405783500778465	0.0
0	27.94592416939	0.0
0	41.0616	0.0
0	48.206	0.0
1	-0.70545056805502837410	0.26816596487157970576
1	-2.0145028385826182272	-0.91594563985411650792
1	-3.17882146596656262	-2.84627255601162901
1	-4.19709693935568	-5.32673986864807
1	-5.07091771510	-8.26819182266
1	-5.80277763	-11.6168375
1	-6.395162	-15.33562
1	-6.850	-19.40
2	-0.0624600582	-0.00235480490
2	-0.7419463	0.2528359
2	-0.5549276	0.04161432
2	-1.522	-0.1790

TABLE III. Complex eigenvalues obtained with $H_{30}^0 = 0$, for $\lambda = 1/2$. Results coincide with the exact ones up to the last digit reported. They have been truncated at 20 significant digits.

straight lines does depend on n , and we have found that in general they move to the right when n increases. Both findings are not surprising: on one hand, for increasing n , the exact eigenfunction is expected to have a larger number of nodes, which increments the number of f_j coefficients that are needed to represent its logarithmic derivative correctly. On the other, for increasing m , the boundary conditions are moved further to the right (i.e., to larger $|r|$), which also increases the number of coefficients needed. As is made apparent by our computations, the effect of the latter is more noticeable. The plots of $\Delta_n(D)$ show that the roots of H_D^d also converge towards the barrier resonances, albeit more slowly. Instead of being straight lines, they are curves that are concave everywhere, except for a number of plateaus which is different for each state. Convergence rate is lower for higher n , meaning that the top curve in the $\lambda = 10$ plot corresponds to Δ_0 , the curve below it corresponds to Δ_1 , and so on. To ease the discussion of these results, we have compiled some logarithmic differences between well and barrier resonances, i.e., $-\log_{10} |\nu_{n^*}^{(m)} - \mu_n|$, in Table V.

m	$\text{Re}(\epsilon)$	$\text{Im}(\epsilon)$
0	24.095880341888706123	0.0
0	39.078924487590608756	0.0
0	54.342383405484864190	0.0
0	70.173203793408790845	0.0
0	86.630901797549645582	0.0
0	103.722769025200	0.0
0	121.4400060068	0.0
0	139.768519	0.0
0	158.693	0.0
1	-10.243001240262833149	6.9319297923706305098
1	-3.7481264282889514022	8.0918634524566962810
1	3.1090702082731894910	6.6772727549801459614
1	-16.525883780702648862	4.1357639513958152182
1	-22.63511276702947437	0.09542171991804396736
1	-28.583717704014	-4.97259427564364
1	-34.3769116736	-10.93053096967
1	-40.017132	-17.682645
1	-45.506	-25.1582
2	-0.0624998	-0.000000526971
2	-3.74812643	8.09186345
2	3.109070208273	6.677272754981
3	-3.748126	8.091863

TABLE IV. Complex eigenvalues obtained with $H_{30}^0 = 0$, for $\lambda = 10$. Results coincide with the exact ones up to the last digit reported. They have been truncated at 20 significant digits.

Focusing first on the curve for Δ_0 , we note that, when $D < 15$, it coincides with $\Delta_{0*}^{(1)}$, which suggests that the solution being obtained is a well resonance, whose eigenvalue coincides with that of a barrier resonance up to approximately 12 decimal places. At $D = 15$, a small region is reached where incrementing D does not seem to improve accuracy; in that region, $\Delta_0 \approx 12.5$ coincides with $-\log_{10}|\epsilon_0 - \epsilon_{0*}^{(1)}|$, implying that $\tilde{\epsilon}_{0*}^{(1)}$ is a more accurate representation of $\epsilon_{0*}^{(1)}$ than $\epsilon_{0*}^{(1)}$ is of ϵ_0 . When $D > 25$, convergence seems to pick up, and the plot of Δ_0 becomes a concave curve with no additional plateaus; i.e., for $D > 25$ and $m > 1$, $\Delta_0 > \Delta_{0*}^{(m)}$. The curve for Δ_1 is similar, but presenting two plateaus; before the first plateau, it coincides with the curve for $\Delta_{1*}^{(1)}$. Then, at the first plateau, located approximately between $D = 15$ and $D = 40$, $\Delta_1 = 8.75$, in coincidence with the entry for $m = 1$, $n = 0$ of Table V. After that, Δ_1 adopts the form of $\Delta_{1*}^{(2)}$, until it reaches a second plateau

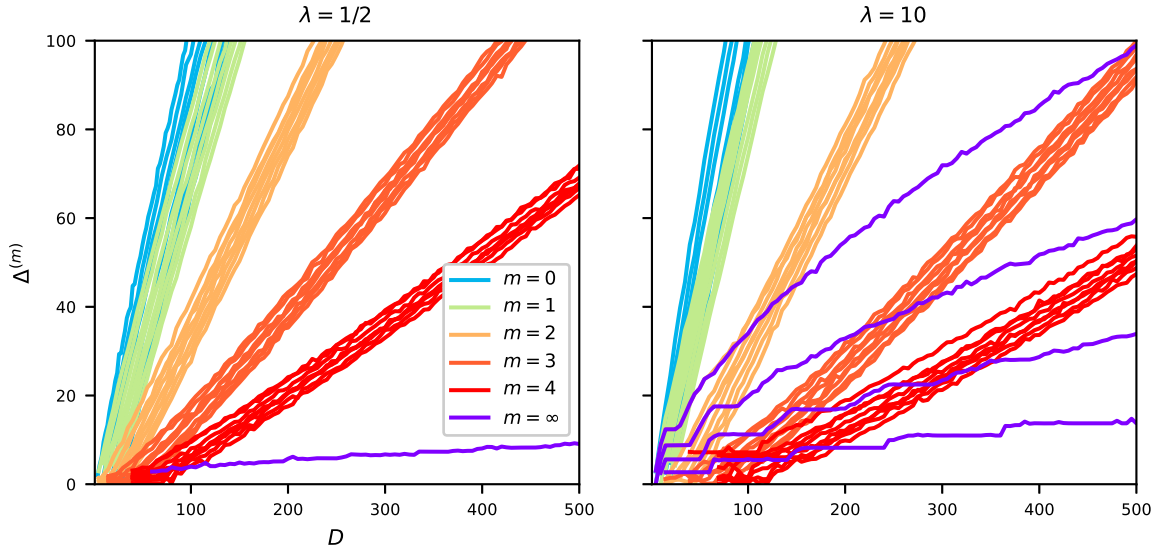


FIG. 3. $\Delta_n^{(m)}(D)$ for $\lambda = 1/2$ and $\lambda = 10$. $m = \infty$ denotes $\Delta_n(D)$, instead.

where $\Delta_1 \approx 17.53$ [c.f. Table V], located in a region where $65 < D < 80$. Finally, it assumes its concave shape, where $\Delta_1 > \Delta_{1*}^{(m)}$, for $m > 2$. Similar explanations can be devised for the curves for Δ_2 , which seems to present four plateaus (all included in Table V), and for Δ_3 , which shows about 5 plateaus, all of them also included in the same table. The plateaus observed in Fig. 3 are quite probably an artificial byproduct of our method to find the roots of H_D^d . It is very likely that there are sequences of roots of the Hankel determinants that coincide with the concave part of the curves we described, but do not have the plateaus nor the parts that match exactly with the curves for well resonances; we are just not able to find them since we do not have good starting points for the NR method.

The results presented above suggest that the roots of the Hankel determinants converge

m	n			
	0	1	2	3
1	12.39	8.75	5.60	2.70
2	24.88	17.53	11.22	5.46
3	37.37	26.30	16.85	8.22
4	49.86	35.07	22.47	10.97
5	62.34	43.85	28.10	13.73

TABLE V. $-\log_{10} |\varepsilon_n - \varepsilon_{n*}^{(m)}|$ for the four states with $\lambda = 10$.

towards both the well and barrier resonances. The authors of Ref. 34 only found the well resonances, since they performed computations with $D \leq 20$, which is not enough to discover the barrier ones.

IV. CONCLUSIONS

We have studied the analytical solutions to the Schrödinger equation with a repulsive exponential potential, as well as those to the Schrödinger equation with an infinite exponential well, and shown that the complex spectra associated to both problems are related as some of the eigenvalues of the latter tend to those of the former when the potential parameter λ increases. Those well resonances that do not tend towards barrier ones do so instead to real fractional numbers. Starting from any of the two problems, if a complex rotation $r = \rho e^{i\theta}$ is performed, then $\theta_{\text{crit}} = \pi/2$ separates one set of resonances from the other. These findings are similar to those of Refs. 7, 8, 41, and 42 regarding the potential proposed by Moiseiev⁴⁰, which had two sets of resonances that were uncovered by complex rotation, separated by $\theta_{\text{crit}} = \pi/4$. In both cases, even though the asymptotic behavior of the solutions is markedly different, the eigenvalues remain quite close to each other.

Regarding the RPM, we have found a satisfactory explanation for the seemingly wrong results obtained in Refs. 28, 31, and 34: all the resonances that are deemed wrong there are in fact well resonances. We have computed the roots of the Hankel determinants and analyzed how they converge towards both the well and barrier resonances, our findings suggesting that there are sequences of them that converge independently to both of their kinds. Contrarily, we were not able to obtain any of the virtual states by means of this method. All of the above suggests that it is only possible to obtain approximations to eigenvalues that are discoverable by a complex rotation, even though the RPM does not require to perform one explicitly. The results obtained in the present work therefore provide evidence that the convergent sequences of roots of the Hankel determinants always correspond to eigenfunctions that decay asymptotically through some path in the complex plane.

ACKNOWLEDGMENTS

This work was funded by Consejo Nacional de Investigaciones Científicas y Técnicas (CONICET).

CONFLICT OF INTEREST STATEMENT

The author has no conflicts to disclose.

DATA AVAILABILITY

The data that support the findings of this study are available from the corresponding author upon reasonable request.

REFERENCES

- ¹A. J. F. Siegert, “On the derivation of the dispersion formula for nuclear reactions,” *Physical Review* **56**, 750–752 (1939).
- ²J. Aguilar and J. M. Combes, “A class of analytic perturbations for one-body Schrödinger Hamiltonians,” *Communications in Mathematical Physics* **22**, 269–279 (1971).
- ³E. Balslev and J. M. Combes, “Spectral properties of many-body Schrödinger operators with dilatation-analytic interactions,” *Communications in Mathematical Physics* **22**, 280–294 (1971).
- ⁴F. M. Fernández and J. Garcia, “On the eigenvalues of some non-Hermitian oscillators,” *Journal of Physics A: Mathematical and Theoretical* **46**, 195301 (2013).
- ⁵A. Kuroś and A. Okopińska, “Two-electron resonances in quasi-one dimensional quantum dots with Gaussian confinement,” *International Journal of Theoretical Physics* **54**, 4164–4173 (2015).
- ⁶T. Myo and K. Katō, “Complex scaling: Physics of unbound light nuclei and perspective,” *Progress of Theoretical and Experimental Physics* **2020**, 12A101 (2020).
- ⁷M. Rittby, N. Elander, and E. Brändas, “Weyl’s theory and the complex-rotation method applied to phenomena associated with a continuous spectrum,” *Physical Review A* **24**, 1636–1639 (1981).

- ⁸M. Rittby, N. Elander, and E. Brändas, “Weyl’s theory and the method of complex rotation,” *Molecular Physics* **45**, 553–572 (1982).
- ⁹O. Atabek, R. Lefebvre, and M. Jacon, “Poles of the scattering amplitude for the repulsive exponential potential: analytic and complex rotation studies,” *Journal of Physics B: Atomic and Molecular Physics* **15**, 2689–2701 (1982).
- ¹⁰O. Atabek and R. Lefebvre, “On the occurrence of multiple spectra of eigenvalues in the one-dimensional complex scaled Schrödinger equation,” *Il Nuovo Cimento B Series 11* **76**, 176–188 (1983).
- ¹¹S. Kais and D. R. Herschbach, “Dimensional scaling for quasistationary states,” *The Journal of Chemical Physics* **98**, 3990–3998 (1993).
- ¹²P. Midy, O. Atabek, and G. Oliver, “Complex eigenenergy spectrum of the Schrödinger equation using Lanczos–tau method,” *Journal of Physics B: Atomic, Molecular and Optical Physics* **26**, 835–853 (1993).
- ¹³C. H. Maier, L. S. Cederbaum, and W. Domcke, “A spherical-box approach to resonances,” *Journal of Physics B: Atomic and Molecular Physics* **13**, L119–L124 (1980).
- ¹⁴S.-G. Zhou, J. Meng, and E.-G. Zhao, “A spherical-box approach for resonances in the presence of the Coulomb interaction,” *Journal of Physics B: Atomic, Molecular and Optical Physics* **42**, 245001 (2009).
- ¹⁵S. A. Sofianos and S. A. Rakityansky, “Exact method for locating potential resonances and Regge trajectories,” *Journal of Physics A: Mathematical and General* **30**, 3725–3737 (1997).
- ¹⁶Z.-D. Bai, Z.-X. Zhong, Z.-C. Yan, and T.-Y. Shi, “Complex coordinate rotation method based on gradient optimization,” *Chinese Physics B* **30**, 023101 (2021).
- ¹⁷N. Yapa, K. Fosse, and S. König, “Eigenvector continuation for emulating and extrapolating two-body resonances,” *Physical Review C* **107**, 064316 (2023).
- ¹⁸O. I. Tolstikhin, V. N. Ostrovsky, and H. Nakamura, “Siegert pseudo-states as a universal tool: Resonances, S-matrix, Green function,” *Physical Review Letters* **79**, 2026–2029 (1997).
- ¹⁹O. I. Tolstikhin, V. N. Ostrovsky, and H. Nakamura, “Siegert pseudostate formulation of scattering theory: One-channel case,” *Physical Review A* **58**, 2077–2096 (1998).
- ²⁰P. A. Batishchev and O. I. Tolstikhin, “Siegert pseudostate formulation of scattering theory: Nonzero angular momenta in the one-channel case,” *Physical Review A* **75**, 062704

- (2007).
- ²¹R. Čurík, M. Tarana, and J. Horáček, “Expansion of scattering length in S-matrix poles and the phenomenon of resistant virtual states,” *Physical Review A* **108**, 012807 (2023).
- ²²U. V. Riss and H. D. Meyer, “Calculation of resonance energies and widths using the complex absorbing potential method,” *Journal of Physics B: Atomic, Molecular and Optical Physics* **26**, 4503–4535 (1993).
- ²³I. B. Müller, R. Santra, and L. S. Cederbaum, “Resonances and pseudoresonances in a potential with attractive coulomb tail: A study using analytic-continuation techniques,” *International Journal of Quantum Chemistry* **94**, 75–92 (2003).
- ²⁴S. A. Rakityansky, S. A. Sofianos, and N. Elander, “Padé approximation of the S-matrix as a way of locating quantum resonances and bound states,” *Journal of Physics A: Mathematical and Theoretical* **40**, 14857–14869 (2007).
- ²⁵L. Zhang, S.-G. Zhou, J. Meng, and E.-G. Zhao, “Real stabilization method for nuclear single-particle resonances,” *Physical Review C* **77**, 014312 (2008).
- ²⁶H. Liang, J. Meng, and S.-G. Zhou, “Hidden pseudospin and spin symmetries and their origins in atomic nuclei,” *Physics Reports* **570**, 1–84 (2015).
- ²⁷F. M. Fernández, “Direct calculation of accurate Siegert eigenvalues,” *Journal of Physics A: Mathematical and General* **28**, 4043–4051 (1995).
- ²⁸F. M. Fernández, “Resonances for a perturbed Coulomb potential,” *Physics Letters A* **203**, 275–278 (1995).
- ²⁹F. M. Fernández, Q. Ma, and R. H. Tipping, “Tight upper and lower bounds for energy eigenvalues of the Schrödinger equation,” *Physical Review A* **39**, 1605–1609 (1989).
- ³⁰F. M. Fernández, Q. Ma, and R. H. Tipping, “Eigenvalues of the Schrödinger equation via the riccati-padé method,” *Physical Review A* **40**, 6149–6153 (1989).
- ³¹F. M. Fernández, “Quantization condition for bound and quasibound states,” *Journal of Physics A: Mathematical and General* **29**, 3167–3177 (1996).
- ³²F. M. Fernández, “Tunnel resonances for one-dimensional barriers,” *Chemical Physics Letters* **281**, 337–342 (1997).
- ³³F. M. Fernández, “The accurate calculation of resonances in multiple-well oscillators,” *Journal of Physics A: Mathematical and Theoretical* **41**, 065202 (2008).
- ³⁴P. Amore and F. M. Fernández, “Accurate calculation of the complex eigenvalues of the Schrödinger equation with an exponential potential,” *Physics Letters A* **372**, 3149–3152

- (2008).
- ³⁵F. M. Fernández, “Accurate calculation of resonances for a central-field model potential,” *Applied Mathematics and Computation* **218**, 5961–5965 (2012).
- ³⁶F. M. Fernández and J. Garcia, “On two different kinds of resonances in one-dimensional quantum-mechanical models,” *Journal of Mathematical Chemistry* **55**, 623–631 (2016).
- ³⁷F. M. Fernández and J. Garcia, “Highly accurate calculation of the resonances in the Stark effect in hydrogen,” *Applied Mathematics and Computation* **317**, 101–108 (2018).
- ³⁸S. T. Ma, “Redundant zeros in the discrete energy spectra in Heisenberg’s theory of characteristic matrix,” *Physical Review* **69**, 668–668 (1946).
- ³⁹D. T. Haar, “On the redundant zeros in the theory of the Heisenberg matrix,” *Physica* **12**, 501–508 (1946).
- ⁴⁰N. Moiseyev, P. Certain, and F. Weinhold, “Resonance properties of complex-rotated Hamiltonians,” *Molecular Physics* **36**, 1613–1630 (1978).
- ⁴¹H. J. Korsch, H. Laurent, and R. Möhlenkamp, “Comment on ”Weyl’s theory and the complex-rotation method applied to phenomena associated with a continuous spectrum”,,” *Physical Review A* **26**, 1802–1803 (1982).
- ⁴²M. Rittby, N. Elander, and E. Brändas, “Reply to ”comment on weyl’s theory and the complex-rotation method applied to phenomena associated with a continuous spectrum”,,” *Physical Review A* **26**, 1804–1807 (1982).
- ⁴³T. mpmath development team, *mpmath: a Python library for arbitrary-precision floating-point arithmetic (version 1.3.0)* (2023), <http://mpmath.org/>.
- ⁴⁴H. Bateman, *Higher transcendental functions*, Vol. 2 (McGRAW-HILL book company, 1953).
- ⁴⁵S. M. Bagirova and A. K. Khanmamedov, “On zeros of the modified Bessel function of the second kind,” *Computational Mathematics and Mathematical Physics* **60**, 817–820 (2020).
- ⁴⁶Y. Krynytskyi, , and A. R. and, “Asymptotic estimation for eigenvalues in the exponential potential and for zeros of $k_{i\nu}$ with respect to order,” *Symmetry, Integrability and Geometry: Methods and Applications* **17**, 057 (2021).
- ⁴⁷DLMF, “*NIST Digital Library of Mathematical Functions*,” <https://dlmf.nist.gov/>, Release 1.1.10 of 2023-06-15, f. W. J. Olver, A. B. Olde Daalhuis, D. W. Lozier, B. I. Schneider, R. F. Boisvert, C. W. Clark, B. R. Miller, B. V. Saunders, H. S. Cohl, and M. A. McClain, eds.

- ⁴⁸S. Abbasbandy and C. Bervillier, “Analytic continuation of Taylor series and the boundary value problems of some nonlinear ordinary differential equations,” *Applied Mathematics and Computation* **218**, 2178–2199 (2011).
- ⁴⁹F. M. Fernández and J. Garcia, “Highly accurate calculation of the real and complex eigenvalues of one-dimensional anharmonic oscillators,” *Acta Polytechnica* **57**, 391 (2017).
- ⁵⁰C. Bauer, A. Frink, and R. Kreckel, “Introduction to the GiNaC framework for symbolic computation within the C++ programming language,” *Journal of Symbolic Computation* **33**, 1–12 (2002).
- ⁵¹J. Vollinga, “GiNaC—symbolic computation with C++,” *Nuclear Instruments and Methods in Physics Research Section A: Accelerators, Spectrometers, Detectors and Associated Equipment* **559**, 282–284 (2006).